Substrate-Rhodium cooperativity in photoinduced ortho-alkynylation of arenes

Argha Saha
IIT BOMBAY
Animesh Ghosh
IIT BOMBAY
Srimanta Guin
IIT BOMBAY
Sanjib Panda
IIT BOMBAY
Dibya Kanti Mal
IIT BOMBAY
Abhirup Majumdar
IIT BOMBAY
Munetaka Akita
Tokyo Institute of Technology
Debabrata Maiti (dmaiti@iitb.ac.in)
Indian Institute of Technology Bombay

Article

Keywords:

Posted Date: June 15th, 2022

DOI: https://doi.org/10.21203/rs.3.rs-1710496/v1

Abstract

In the realm of metallaphotocatalytic C-H activation strategy, the mode of reaction which has been mostly explored is the synergistic effect between a photocatalyst (PC) and a transition metal. In these cases, the energy and redox transfer from the PC to transition metal modulates the oxidation state which brings new mechanistic paradigms in C-H activation and enables prior elusive transformations under milder conditions. Another mode of reactivity occurs via the direct excitation of the transition metal which plays the dual role of light energy harnessing alongside performing the bond breaking and forming. This mode is advantageous because it would not require any exogenous PC, however such reactivity by transition metals is rare in literature. In this context we have developed the first photo-induced Rh-catalyzed ortho-alkynylation under ambient conditions without the requirement of silver salt, PC or any engineered substrate or catalyst. The transformation functions by the specific cooperative effect of a six-membered rhodacycle which is the photo-responsive species. The catalytic system allows the conjugation of arenes with sp3-rich pharmacophoric fragments. The control experiments as well as the computational studies resolve the mechanistic intricacies for this transformation. An outer sphere electron transfer process from Rh to alkynyl radical is operative for the present photo-induced transformation over the more common oxidative addition or 1,2-migratory insertion pathways.

Main Text

The C-H activation strategy gives the provision to streamline the overall process toward a target molecule; thereby empowering the genre of organic synthesis.[1] However, it is a general convention that for a thermally induced C-H activation, a transition metal catalyst is usually accompanied with stoichiometric silver or copper oxidants.[2] This questions the practicality of the method. In order to harness the applicability in true terms it is required to utilize an alternative energy resource that would provide the same outcome but in a sustainable manner.[3] This is where the merger of transition metal catalysis and photocatalysis fits in aptly. The metallaphotocatalysis is an expanding domain in organic synthesis that has revisited and recreated the traditional modes of transition metal catalyzed reactions via unorthodox open-shell mechanisms.[4] The metallaphotocatalysis functions by leveraging on the modulated oxidation state of metal complex involved or generating excited form of intermediate catalytic species; which accounts for the key organometallic step of the transformation.[5] Thus, metallaphotocatalysis provides access to unique reactivity modes through entirely new mechanistic paradigms, that complements the conventional mechanistic approach in the realm of transition metal catalysis. The redefined mechanistic features enabled by metallaphotocatalysis allow the accomplishment of prior elusive transformations.

In general, the metallaphotocatalysis operates by two distinct modes. The first mode constitutes of the synergistic cooperativity between a transition metal and a photosensitizer that display a dual catalytic manifold (Figure 1a, left).[6] This mode of the reaction pathway is more pronounced and is amenable to a plethora of C-H functionalization protocols. In this context, the Rh/PC conjugation has been employed recently to achieve intriguing reactivity under ambient conditions (Figure 1b).[7] The ligation of

photosensitizer to the cyclopentadienyl (Cp) ligand of Rh catalyst provides a bimodular catalyst that enables the *ortho*-C–H arylation and alkylation of arenes. This conjugate functions via the photoinduced intramolecular metal to ligand charge transfer, that generates the cationic CpRh(IV) and lowers the energy for the product formation step by a faster reductive elimination. On a contrary, very recently *ortho*-borylation has been achieved which proceeds via the low valent rhodate (II) anionic complex by a one electron reduction of Rh(III) from the Ir based photocatalyst (Figure 1c).[8] The formation of anionic complex facilitates the interaction with electron deficient boron, that makes the photo-induced *ortho*-C-H borylation feasi-ble under mild conditions.

The second mode of reaction path is distinct from the above-mentioned paradigm and constitutes of only transition metal catalysis that harness the photon energy and catalyze the reaction sequences, obviating the requirement of an exogeneous photosensitizer (Figure 1a, right).[6] This dual mode of reactivity was demonstrated for Ru(II)-catalyzed C–H *meta*-alkylation, where photo-induced homolysis of alkyl bromide produces the alkyl radical which in turn drives the oxidation of Ru(II) complex to cationic Ru(III).[9] In our recent report, we have shown that Pd can also be employed in a similar fashion to effectuate the highly regioselective Fujiwara-Moritani reaction.[10] Although uncommon with Rh catalysis, but with an engineered *N*-heterocyclic carbene–Rh(I) catalyst it is possible to self-drive the photo-induced *ortho*-borylation process (Figure 1d).[11] Alike a borylation process, introducing an alkynyl group into arenes is of utmost importance because of the highly transformable nature of the alkyne functionality.[12,13] Pertaining to advancement of photo-induced Rh catalyzed C-H functionalization, in the present report, we have demonstrated a substrate-Rh cooperative reactivity that enable the inverse Sonogashira reaction[14] at *ortho*-position of arenes without any sophistication in catalysts or substrates designing (Figure 1e). Noteworthy, the present protocol allows the C-H alkynylation under a silver-free conditions which is otherwise a prime requirement for a similar thermally induced transformation.[15] To the best of our knowledge, this constitutes the first example of photo-induced Rh catalyzed *ortho*-alkynylation under silver free conditions.

The selection of substrate is an important aspect of the present transformation since the substrate/Rh complex has to potentially harness the light energy in visible region to enable cooperativity effect towards *ortho*-alkynylation. To commence with, 2-phenylpyridine, which has been employed previously for photo-induced Rh catalyzed C-H functionalizations, was chosen as the model substrate. A mixture consisting of $[Rh(COD)Cl]_2$ and 2-phenylpyridine (1:1) was irradiated with blue light. A UV-vis study of the irradiated substrate-catalyst adduct suggested that the complex shows no absorption in visible light region (l_{max} 297 nm) (Figure 1f, I). Hence, to further red-shift the absorption value towards the visible light region, benzo-[*h*]-quinoline was chosen as the substrate and the identical experimental sets were carried out. However, the l_{max} value (349 nm) for this adduct indicated that it is unlikely to cause any absorption in visible region (Figure 1f, II). A similar inference could be made for 2-phenylquinoline as substrate based on its l_{max} value (328 nm) (Figure 1f, III). Surprisingly, with 8-naphthylquinoline, which is expected to form a six-membered rhodacycle, a large shift in absorption peaks were observed (l_{max} 490 nm) in comparison

to the parent substrate (Figure 1f, IV see supplementary information, section 6 for full details). Though the individual precursors $[Rh(COD)Cl]_2$ or 8-(naphthalen-1-yl)quinoline failed to exhibit any significant absorption band at the visible region, but their *in situ* generated Rh-substrate adduct strongly absorbs light at ~490 nm. Multiple absorptions of the adduct in the UV-vis region have also been analyzed by time-dependent density functional (TD-DFT) formalism (Figure 1g) in which the lowest energy absorption band at ~490 nm is originated via the MLCT (dp of Rh(I) ®p* of L) transition. Hence, from the present study it may be concluded that for the substrate/Rh synergistic effect to be feasible a six-membered rhodacycle is a primary requirement over the more favored five-membered metallacycle. This was further confirmed by the ^1H NMR studies, which in case of 8-(naphthalen-1-yl)quinoline /Rh adduct exhibited a complete alteration of the signals in comparison to the parent substrate upon irradiation (see supplementary information, section 7 for full details). While in case of 2-phenylpyridine only a subtle change in signals were ob-served even after being irradiated for 24 h (see supplementary information, section 7 for full details). Based on this analysis, 8-naphthylquinoline was chosen as the substrate to execute the photo-induced *ortho*-alkynylation with (bromoethynyl)triisopropylsilane in presence of $[Rh(COD)Cl]_2$ / $KHCO_3$ / acetic acid combination (see supplementary information, section 2.2 for full details). The formation of desired *ortho*-alkynylated product **1** (30% yield by GC analysis) in absence of the silver salt oxidant or an exogenous photosensitizer proved that with a proper selection of substrate it is possible to conduct C-H activation only through substrate-catalyst cooperativity. The product structure **1** was characterized by spectroscopic techniques and further confirmed by X-ray crystallography (CCDC 2103199). The same reaction with 2-phenylpyridine did not afford any product as was expected from the UV-vis studies. The reaction in absence of light was completely silent justifying the role of light in promoting the transformation. The aforementioned condition was not amenable to other Rh, Ru and Ir catalyst except for $Rh(COD)Cl]_2$ (see supplementary information, section 2.2 for full details). The other reaction parameters were optimized which revealed that replacing $KHCO_3$ with KH_2PO_4 (2 equiv.) and prolonging the reaction time to 24 h rendered 1 in a vastly improved yield (86% by GC analysis). It may be noted that the internal temperature of the reaction vial lied between 30 ^oC to 35 ^oC as was monitored throughout the reaction time. The requirement of a six-membered rhodacycle to enable the *ortho*-alkynylation has also been further confirmed by an intermolecular competition experiment. When an equimolar ratio of 2-phenylpyridine and 8-naphthylquinoline were subjected to alkynylation under the optimized conditions, only product **1** was formed although the yield was low in comparison to the optimized yield (Figure 1h). The reduction in yield could be attributed to the catalytic impediment by 2-phenylpyridine. Also, a 1:1 Rh-8-naphthylquinoline mixture upon irradiation with blue light followed by subsequent reaction with (bromoethynyl)triisopropylsilane gave the desired product **1** in 71% yield; suggesting the pivotal role of the *in situ* generated adduct in execution of the present transformation. Details of the optimization studies and control experiments are provided in Supplementary Information (see supplementary information, section 2.2 and 4.1 for full details).

The attainment of optimal conditions for photo-induced Rh catalyzed *ortho*-alkynylation of 8-naphthylquinoline was pursued further towards generalizing the scope of the transformation (Figure 2). The alkynyl variants with different substitution pattern at the silyl group were explored initially, which

provided the anticipated alkynylated products (**2** and **3**) in good yields. The nucleophilic addition of alkynyl magnesium bromides into ketones lead to the formation of propargyl alcohols which can be further converted to their corresponding silyl ethers.[13e,16] A series of these propargyl silyl ethers were targeted for photo-induced *ortho*-alkynylation (Figure 2). The alkynyl bromide derived from cyclopropyl methyl ketone, cyclopentanone and cyclohexanone respectively underwent facile reaction affording the cycloalkane conjugated alkynylated products (**4**, **5** and **6**) in good yields. The transformation is also feasible with various substituted cyclohexane linked alkynyl bromides (**7**-**9**). The alkynyl bromides from bicyclic alkanone viz. norbornanone and heterocyclic based ketone viz. pyranone were also found to be suitable as substrates to be incorporated at the *ortho*-position of arenes in synthetically useful yields (**10** and **11**). The transformation could also engage in various propargyl silyl ethers possessing larger ring systems (7, 8, 12 and 15-membered) (**12**-**15**) to provide their corresponding products. The structure of compound **14** was confirmed by X-ray crystallography (CCDC 2168677). Apart from cyclo-alkanones, the reactions with the propargyl silyl ethers from benzophenone (**16**) and acyclic ketone viz. methyl iso-propyl ketone (**17**) also proceeded smoothly under the present photo-induced reaction conditions, which are generally deemed as difficult substrates in the alkynylation process. The suitability of the present transformation to a variety of cycloalkyl linked propargyl silyl ethers prompted to venture on the carbonyl-containing sp^3-rich natural product fragments. The milder nature of the present photo-induced inverse Sonogashira allows a range of pharmaceutically relevant and biologically active ketones e.g. estrone (**18**), menthone (**19**), epiandrosterone (**20**), camphor (**21**) and fenchone (**22**) to be covalently linked to arenes.

We next evaluated the scope of DG possessing arenes having electronically diverse substituents in the arene part (Figure 3). With alkyl substituents at the *ortho*-position high yields of corresponding alkynylated products (**23**-**25**) were obtained. The presence of bulky iso-propyl group (**25**) did not hamper the reactivity. Even free phenol group was tolerated in this transformation without the requirement of prior protection (**26**). Substrates with ether (**27** and **28**), trifluoromethyl (**29** and **30**), esters (**31**) and alkyl esters (**32** and **33**) functional groups at the *ortho*-position were viable substrates to afford the desired alkynylated products in decent yields upon reaction with triisopropylsilyl acetylene or propargyl silyl ethers. Noteworthy, the ester functionality (**31**-**33**) was left untouched under the acidic conditions employed for this transformation. With 1,2- and 1,3- di-substitution pattern in the arenes, the photo-induced alkynylation occurred smoothly with synthetically useful yields of their corresponding products (**34**-**40**) irrespective of the electronic and steric nature of the substituents present. The tri-substituted arenes was also compatible to the photo-irradiated alkynylation process to render the ortho-alkynylated product (**41**) in decent yield. Further, the alkynylation process could be executed on various C4-substituted naphthyl (**42**-**45**), acenaphthenyl (**46**) and pyrenyl (**47** and **48**) substrates. The tethering of drug molecule flurbiprofen (**49**) or natural products menthol and fenchol (**50** and **51**) to the arenes did not impede the reactivity of the substrate towards alkynylation. This showcases the robustness of the present protocol in accommodating a wide substrate range with high tolerance to different functional groups. However, with *para*-substituted arenes, the di-alkynylation occurred predominantly over the mono-alkynylation (**52**-**54**).

The same observation was made for the heterocyclic substrate quinoline giving rise to di-alkynylation at C5 and C7 position (**55**).

The transformable nature of the alkynyl moiety in the synthesized *ortho*-alkynylated arenes products led us to conduct a series of functional group conversion (Figure 4). Product **31** when subjected to ruthenium catalyzed oxidation in presence of sodium periodate gave the corre-sponding carboxylic acid ester **56**. While the product **1** upon treatment with tert-butyl nitrite and TEMPO afforded the 1,2-addition product **57** in high yield. The desilylation of **1** with CsF gave **58**. Subsequently, reaction of isolated **58** with tert-butyl nitrite in presence of picoline-*N*-oxide gave the *ortho*-cyano derivative **59** while the desilylated product of **23** under ruthenium catalyzed oxidation in presence of tert-butyl hydroperoxide transformed the alkynyl moiety to a formyl derivative **60**. The synthetic utility of the protocol was further demonstrated by conducting a gram scale reaction that provided an acceptable yield of the product (Figure 4b).

We next delved into the mechanistic aspects of the photo-induced alkynylation under silver free conditions. To probe if any radical is involved in this transformation, alkynylation reaction was performed in presence of TEMPO (2,2,6,6-tetramethylpiperidine-1-oxyl), butylated hydroxytoluene (BHT) and phenyl *N*-tert-butylnitrone (PNB). With three equivalence of the radical inhibitor reagents, the reaction proceeded with noticeable decrease of catalytic activities while with five equivalence the reactions were impede to large extent giving only traces of the product **1** (Figure 5a, see supplementary information, section 4.1 for details). The impediment of reaction suggests the generation of a radical species in the reaction. When alkynyl bromide was irradiated with blue light in presence of the radical scavenger TEMPO, the formation of the corresponding TEMPO-alkyne adduct (**61**) formation was observed by mass analysis (Figure 5b, see supplementary information, section 4.1 for details). Also, alkynyl bromide under the blue light irradiation provided the diyne (**62**). But the same diyne formation did not occur in absence of light even in the presence of Rh catalyst (Figure 5c, see supplementary information. Section 4.1 for details). These observations indicate that the *ortho*-alkynylation most likely goes via the initial homolysis of the alkynyl bromide to alkynyl radical.[17] The photo-irradiated C–H activation by Rh(I) is documented in literature; however, the intriguing aspect was how the substrate-Rh cooperativity enables the *ortho*-alkynylation by engaging the *in situ* generated alkynyl radical. In order to gain an insight on the aforesaid, computational studies were carried out (Figure 5d, see supplementary information, section 9 for details). The study suggest that initial C–H activation of the 8-(naphthalen-1-yl)quinoline leads to the photo-responsive six-membered rhodacycle **A** ([RhI(L)(COD)], S_0). Absorption of visible light (I_{max} = 490 nm) stimulates the excitation of **A** (S_0) to ***A** (S_1) (Figure 5d), which is decayed through inter-system crossing (ISC) to generate triplet species **B** (^{3}A, T_1). The homolysis of (bromoethynyl)triisopropylsilane generates the alkynyl and bromide radicals. The formation of high energy radical species prompts the meta-stable ^{3}A to participate in the electron transfer process. Two simultaneous single electron transfer from Rh(I) by an outer sphere mechanism leads to the formation of alkynyl and bromide anions along with the concomitant oxidation of the catalyst to Rh(III). The alkynyl anion ligates to Rh(III) and enter into the coordination sphere of Rh resulting in intermediate **C** by overcoming a high energy barrier at ambient condition. This has been experimentally confirmed by order studies which suggest the involvement of

substrate, alkyne and Rh catalyst in the rate determining step (see supplementary information, section 4.3 for details). Also, the kinetic isotope effect studies suggest that the C–H activation is not the energy demanding step of the transformation (see supplementary information, section 4.2 for details). It may be noted that under the similar thermally induced process, it is usually the oxidative addition or the 1,2-migratory insertion of the catalyst into alkynyl bromide that is favored. A difference in the mechanism operative forges the present transformation under mild conditions in absence of any silver salt as an oxidant. Further, an intramolecular rearrangement (**D**) followed by reductive elimination of the alkynylated 8-(naphthalen-1-yl)quinoline derivative restores the catalyst $[Rh(COD)Cl]_2$.

In summary, we have devised the first protocol on a photo-induced Rh catalyzed *ortho*-alkynylation under silver free conditions. With the proper substrate choice, where Rh can form a six-membered rhodacycle enables the transformation by harnessing the photo-chemical energy. The transformation does not require any sophistication engineering in either catalyst or substrate. With the aid of substrate-Rh cooperativity it is possible to effectuate both the activation of $C(sp^2)$-H bond as well as the C-alkyne bond formation under ambient conditions. The transformation is amenable with different alkyne variants, to the extent of incorporation of various pharmacologically relevant molecules into the arenes by means of alkyne bridge. The mechanistic investigation alongside computational studies shed light about the possible pathway for this transformation. Computational studies suggest that the photo-excited Rh species is responsible for the electron transfer to the high energy alkynyl radical generated *in situ* in the medium by an outer sphere mechanism rather than the more common oxidative addition or 1,2-migratory insertion pathways. The computational findings are in sync with the experimental observations.

Received (to be inserted automatically)

References

1. For selected publications and reviews, see: (a) McMurray, L.; O'Hara, F.; Gaunt, M. J. Recent Developments in Natural Product Synthesis using Metal-Catalysed C–H Bond Functionalisation. *Chem. Soc. Rev.* **40**, 1885–1898 (2011). (b) Abrams, D. J.; Provencher, P. A.; Sorensen, E. J. Recent Applications of C–H Functionalization in Complex Natural Product Synthesis. *Chem. Soc. Rev.* **47**, 8925–8967 (2018). (c) Liu, Y.; Ge, H. Site-selective C–H Arylation of Primary Aliphatic Amines Enabled by a Catalytic Transient Directing Group. *Nat. Chem*. **9**, 26–32 (2017). (d) Roughley, S. D.; Jordan, A. M. The Medicinal Chemist's Toolbox: An Analysis of Reactions used in the Pursuit of Drug Candidates. *J. Med. Chem.* **54**, 3451–3479 (2011). (e) Barker, A.; Kettle, J. G.; Nowak, T.; Pease, J. E. Expanding Medicinal Chemistry Space. *Drug Discovery Today*. **18**, 298–304 (2013). (f) Boström, J.; Brown, D. G.; Young, R. J.; Keserü, G. M. Expanding the Medicinal Chemistry Synthetic Toolbox. *Nat. Rev. Drug Discovery*. **17**, 709–727 (2018). (g) Wencel-Delord, J.; Glorius, F. C–H Bond Activation Enables the Rapid Construction and Late-stage Diversification of Functional Molecules. *Nat. Chem.* **5**, 369–375 (2013). (h) Cernak, T.; Dykstra, K. D.; Tyagarajan, S.;

Vachal, P.; Krska, S. W. The Medicinal Chemist's Toolbox for Late Stage Functionalization of Drug-like Molecules. *Chem. Soc. Rev.* **45**, 546–576 (2016).

2. For selected publications and reviews, see: (a) Chen, Z.; Wang, B.; Zhang, J.; Yu, W.; Liu, Z.; Zhang, Y. Transition metal-catalyzed C–H bond functionalizations by the use of diverse directing groups. *Org. Chem. Front.* **2**, 1107–1295 (2015). (b) Sinha, S. K.; Guin, S.; Maiti, S.; Biswas, J. P.; Porey, S.; Maiti. D. Toolbox for Distal C–H Bond Functionalizations in Organic Molecules. *Chem. Rev.* **122**, 5682–5841 (2022). (c) Rej, S.; Chatani, N. Rhodium-Catalyzed C(sp^2)- or C(sp^3)-H Bond Functionalization Assisted by Removable Directing Groups. *Angew. Chem. Int. Ed.* **58**, 8304–8329 (2019). (d) Bhattacharya, T.; Dutta, S.; Maiti, D. Deciphering the Role of Silver in Palladium-Catalyzed C–H Functionalizations. *ACS Catal.* **11**, 9702–9714 (2021). (e) Bay, K. L.; Yang, Y.-F.; Houk, K. N. Multiple roles of silver salts in palladium-catalyzed C–H activations. *J. Organomet. Chem.* **864**, 19–25 (2018). (f) Lotz, M. D.; Camasso, N. M.; Canty. A. J.; Sanford, M. S. Role of Silver Salts in Palladium-Catalyzed Arene and Heteroarene C–H Functionalization Reactions. *Organometallics* **36**, 165–171 (2017). (g) Bangaru Bhaskararao, B.; Singh, S.; Anand, M.; Verma, P.; Prakash, P.; C, A.; Malakar, S.; Schaefer, H. F.; Sunoj, R. B. Is silver a mere terminal oxidant in palladium catalyzed C–H bond activation reactions? *Chem. Sci.* **11**, 208–216 (2020).

3. (a) Dalton, T., Faber, T., Glorius, F. C–H Activation: Toward Sustainability and Applications. *ACS Cent. Sci*. **7**, 245–261 (2021). (b.) Crisenza, G. E. M.; Melchiorre, P. Chemistry glows green with photoredox catalysis. *Nat. Commun*. **803** (2020).

4. For selected publications and reviews, see: (a) Twilton, J.; Le, C. C.; Zhang, P.; Shaw, M. H.; Evans, R. W.; MacMillan, D. W. C. The merger of transition metal and photocatalysis. *Nat. Rev. Chem*. **1**, 0052 (2017). (b) Buzzetti, L.; Crisenza, G. E. M.; Melchiorre, P. Mechanistic studies in photocatalysis. *Angew. Chem. Int. Ed*. **58**, 3730–3747 (2019). (c) Ravelli, D., Protti, S., Fagnoni, M. Carbon–Carbon Bond Forming Reactions via Photogenerated Intermediates. *Chem. Rev*. **116**, 9850–9913 (2016). (d) Wang, C. S., Dixneuf, P. H., Soulé, J. F. Photoredox Catalysis for Building C–C Bonds from C(sp^2)-H Bonds. *Chem. Rev*. **118**, 7532–7585 (2018). (e) Chan, A. Y., Perry, I. B., Bissonnette, N. B., Buksh, B. F., Edwards, G. A., Frye, L. I., Garry, O. L., Lavagnino, M. N., Li, Y. B .X, Liang, Mao, E., Millet, A., Oakley, J. V., Reed, Nic. L., Sakai, H. A., Seath, C. P., MacMillan, D. W. C. Metallaphotoredox: The Merger of Photoredox and Transition Metal Catalysis. *Chem. Rev*. **122**, 1485–1542 (2022). (f) Douglas, N. H., Nicewicz, D. A. Photoredox-Catalyzed C–H Functionalization Reactions. *Chem. Rev*. **122**, 1925–2016 (2022).

5. For selected publications and reviews, see: (a) Terrett, J. A.; Cuthbertson, J. D.; Shurtleff, V. W.; Mac-Millan, D. W. C. Switching on elusive organometallic mechanisms with photoredox catalysis. *Nature* **524**, 330–334 (2015). (b) Corcoran, E. B.; Pirnot, M. T.; Lin, S.; Dreher, S. D.; Di-Rocco, D. A.; Davies, I. W.; Buchwald, S. L.; MacMillan, D. W. C. Aryl amination using ligand-free Ni(II) salts and photoredox catalysis. *Science* **353**, 279–283 (2016). (c) Le, C.; Chen, T. Q.; Liang, T.; Zhang, P.; MacMillan, D. W. C. A radical approach to the copper oxidative addition problem: Trifluoromethylation of bromoarenes. *Science* **360**, 1010–1014 (2018). (d) Zuo, Z.; Cong, H.; Li, W.; Choi, J.; Fu, G. C.; MacMillan, D. W. C. Enantioselective decarboxylative arylation of α-amino acids via the merger of photoredox and nickel catalysis. *J. Am.*

Chem. Soc. **138**, 1832–1835 (2016). (e) Huo, H.; Shen, X.; Wang, C.; Zhang, L.; Röse, P.; Chen, L.-A.; Harms, K.; Marsch, M.; Hilt, G.; Meggers, E. Asymmetric photoredox transition-metal catalysis activated by visible light. *Nature* **515**, 100–103 (2014). (f) Schweitzer-Chaput, B.; Horwitz, M. A.; de Pedro Beato, E.; Melchiorre, P. Photochemical generation of radicals from alkyl electrophiles using a nucleophilic organic catalyst. *Nat. Chem*. **11**, 129–135 (2019). (g) Huang, H.-M.; Koy, M.; Serrano, E.; Pflüger, P. M.; Schwarz, J. L.; Glorius, F. Catalytic radical generation of π-allylpalladium complexes. *Nat. Catal*. **3**, 393–400 (2020). (i) Ham, J. S.; Park, B.; Son, M.; Roque, J. B.; Jurczyk, J.; Yeung, C. S.; Baik, M.-H.; Sarpong, R. C–H/C–C functionalization approach to N-fused heterocycles from saturated azacycles. *J. Am. Chem. Soc*. **142**, 13041–13050 (2020). (j) Huang, H. M.; Bellotti, P.; Pflüger, P, M.; Schwarz, J. L.; Heidrich, B.; Glorius, F. Three-Component, Interrupted Radical Heck/Allylic Substitution Cascade Involving Unactivated Alkyl Bromides. *J. Am. Chem. Soc*. **142**, 10173–10183 (2020). (k) Zhao, G.; Yao, B W.; Mauro, J. N.; Ngai, M. Y. Excited-State Palladium-Catalyzed 1,2-Spin-Center Shift Enables Selective C-2 Reduction, Deuteration, and Iodination of Carbohydrates. *J. Am. Chem. Soc*. **143**, 1728–1734 (2021). (l) Guillemard, L.; Wencel-Delord, J. When metal-catalyzed C–H functionalization meets visible-light photocatal-ysis. Beilstein *J. Org. Chem*. **16**, 1754–1804 (2020). (m) Chuentragool, P.; Kurandina, D.; Gevorgyan, V. Catalysis by visible light photoexcited palladium complexes. *Angew. Chem. Int. Ed*. **58**, 11586–11598 (2019). (n) Torres, G. M.; Liu, Y.; Arndtsen, B. A. A dual light-driven palladium catalyst: Breaking the barriers in carbonylation reactions. *Science* **368**, 318–323 (2020). (o) Bellotti, P.; Koy, M.; Gutheil, C.; Heuvel, S.; Glorius, F. Three-component three-bond forming cascade via palladium photoredox catalysis. *Chem. Sci*. **12**, 1810-1817 (2021). (p) Fabry, D. C.; Zoller, J.; Raja, S.; Rueping, M. Combining rhodium and photoredox catalysis for C–H functionalizations of arenes: Oxidative Heck reactions with visible light. *Angew. Chem. Int. Ed*. **53**, 10228–10231 (2014). (q) Zoller, J., Fabry, D. C., Ronge, M. A.; Rueping, M. Synthesis of indoles using visible light: photoredox catalysis for palla-dium-catalyzed C–H activation. *Angew. Chem. Int. Ed*. **53**, 13264–13268 (2014). (r) Cheng, W.-M; Shang, R. Transition Metal-Catalyzed Organic Reactions under Visible Light: Recent Developments and Future Perspectives. *ACS Catal*. **10**, 9170–9196 (2020). (s) Prier, C. K.; Rankic, D. A.; MacMillan, D. W. C Visible Light Photoredox Catalysis with Transition Metal Complexes: Applications in Organic Synthesis. *Chem. Rev*. **113**, 5322–5363 (2013). (t) Min, X. T., Ji, D. W., Guan, Y. Q., Guo, S. Y., Hu, Y. C., Wan, B., Chen. Q. A. Visible Light Induced Bifunctional Rhodium Catalysis for Decarbonylative Coupling of Imides with Alkynes. *Angew. Chem. Int. Ed*. **60**, 1583 –1587 (2021).

6. (a) Cheung, K. P. S., Sarkar, S., Gevorgyan, V. Visible Light-Induced Transition Metal Catalysis. *Chem. Rev.* **122**, 1543–1625 (2022). (b) Parasram, M., Gevorgyan, V. Visible light-induced transition metal-catalyzed transformations: beyond conventional photosensitizers. *Chem. Soc. Rev*. **46**, 6227–6240 (2017).

7. Kim, J.; Kim, D.; Chang, S. Merging Two Functions in a Single Rh Catalyst System: Bimodular Conjugate for Light-Induced Oxidative Coupling. *J. Am. Chem. Soc*. **142**, 19052–19057 (2020).

8. Tanaka, J., Nagashima, Y., A. J. A., Dias, A. J. A., Tanaka, K. Photo-Induced ortho-C–H Borylation of Arenes through In Situ Generation of Rhodium(II) Ate Complexes. *J. Am. Chem. Soc*. **143**, 11325–11331 (2021).

9. (a) Gandeepan, P.; Koeller, J.; Korvorapun, K.; Mohr, J.; Ackermann, L. Visible-Light-Enabled Ruthenium-Catalyzed meta- C–H Alkylation at Room Temperature. *Angew. Chem., Int. Ed.* **58**, 9820–9825 (2019). (b) Sagadevan, A.; Greaney, M. F. meta-Selective C–H Activation of Arenes at Room Temperature Using Visible Light: Dual-Function Ruthenium Catalysis. *Angew. Chem., Int. Ed*. **58**, 9826–9830 (2019).

10. Saha, A., Guin, S., Ali, W., Bhattacharya, T., Sasmal, S., Goswami, N., Prakash, G., Sinha, S. K., Chandrashekar, H.B., Panda, S., Anjana, S. S., Maiti. D. Photoinduced Regioselective Olefination of Arenes at Proximal and Distal Sites. *J. Am. Chem. Soc*. **144**, 1929–1940 (2022).

11. Thongpaen, J.; Manguin, R.; Dorcet, V.; Vives, T.; Duhayon, C.; Mauduit, M.; Baslé, O. Visible Light Induced Rhodium(I)-Catalyzed C–H Borylation. *Angew. Chem., Int. Ed*. **58**, 15244–15248 (2019).

12. Diederich, F.; Stang, P. J.; Tykwinski, R. R. *Acetylene Chemistry: Chemistry, Biology and Material Science*; Wiley-VCH: Weinheim, Germany, (2005).

13. For selected publications and reviews, see: (a) Tobisu,M.; Ano, Y.; Chatani, N. Palladium-catalyzed Direct Alkynylation of C–H Bonds in Benzenes. *Org. Lett*. **11**, 3250–3252 (2009). (b) Viart, H. M.-F.; Bachmann, A.; Kayitare, W.; Sarpong, R. β-Carboline Amides as Intrinsic Directing Groups for C(sp^2)-H Functionalization. *J. Am. Chem. Soc*. **139**, 1325–1329 (2017). (c) Ruan, Z.; Sauermann, N.; Manoni, E.; Ackermann, L. Manganese-catalyzed C–H Alkynylation: Expedient Peptide Synthesis and Modification. *Angew. Chem., Int. Ed*. **56**, 3172–3176 (2017). (d) Wang, P.; Li, G.-C.; Jain, P.; Farmer, M. E.; He, J.; Shen, P.-X.; Yu, J.-Q. Ligand-promoted meta-C–H Amination and Alkynylation. *J. Am. Chem. Soc*. **138**, 14092–14099 (2016). (e) Porey, S., Zhang, X., Bhowmick, S., Singh, V. K., Guin, S., Paton, R. S., Maiti. D. Alkyne Linchpin Strategy for Drug:Pharmacophore Conjugation: Experimental and Computational Realization of a Meta-Selective Inverse Sonogashira Coupling. *J. Am. Chem. Soc*. **142**, 3762–3774 (2020). (f) Sasmal, S., Prakash, G., Dutta, U., Laskar, R., Lahiri, G. K., Maiti. D. Directing Group Assisted Rhodium Catalyzed meta-C-H Alkynylation of Arenes. *Chem. Sci*. DOI: 10.1039/D2SC00982J (2022). (g) de Haro, T.; Nevado, C. Gold-Catalyzed Ethynylation of Arenes. *J. Am. Chem. Soc*. **132**, 1512–1513 (2010). (h) Brand, J. P.; Waser, J. Para-selective Gold-catalyzed Direct Alkynylation of Anilines. *Org. Lett*. **14**, 744–747 (2012). (i) Mondal, A.; Chen, H.; Flämig, L.; Wedi, P.; van Gemmeren, M. Sterically Controlled Late-Stage C–H Alkynylation of Arenes. *J. Am. Chem. Soc*. **141**, 18662–18667 (2019). (j) Sarala, A. S., Bhowmick, S., de Carvalho, R. L., Al-Thabaiti, S. A., Mokhtar, M., Eufrânio da Silva Júnior, N., Maiti, D. Transition-Metal-Catalyzed Selective Alkynylation of C-H Bonds. *Adv. Synth. Catal*. **363**, 4994– 5027 (2021).

14. Trofimov, B. A.; Stepanova, Z. V.; Sobenina, L. N.; Mikhaleva, A. I.; Ushakov, I. A. Ethynylation of Pyrroles with 1-Acyl-2-bromoacetylenes on Alumina: A Formal “Inverse Sonogashira Coupling. *Tetrahedron Lett*. **45**, 6513–6516 (2004).

15. For selected publications, see: (a) Xie, F., Qi, Z., Yu, S., Li, X. Rh(III)- and Ir(III)-Catalyzed C–H Alkynylation of Arenes under Chelation Assistance. *J. Am. Chem. Soc.* **136**, 4780–4787 (2014). (b)

Zhang, X., Qi, Z., Gao, J., Li, X. Rhodium(III)-catalyzed C–H alkynylation of azomethine ylides under mild conditions *Org. Biomol. Chem*. **12**, 9329–9332 (2014). (c) Feng, C., Loh, T.-P. Rhodium-Catalyzed C-H Alkynylation of Arenes at Room Temperature *Angew. Chem. Int. Ed*. **126**, 2760–2764 (2014). (d) Wang, S.-B., Gu, Q., You, S.-L. Rhodium(III)-Catalyzed C–H Alkynylation of Ferrocenes with Hypervalent Iodine Reagents *J. Org. Chem*. **82**, 11829–11835 (2017). (d) Tan, E., Quinonero, O., de Orbe, M. E., Echavarren, A. M. Broad-Scope Rh-Catalyzed Inverse-Sonogashira Reaction Directed by Weakly Coordinating Groups. *ACS Catal*. **8**, 2166–2172 (2018). (e) Tan, E., Magraner, M. M., Morales, C. G., Mayansab, J. G., Echavarren, A. M. Rhodium-catalysed ortho-alkynylation of nitroarenes. *Chem. Sci*., **12**, 14731–14739 (2021). (f) Tan, E., Nannini, L. J., Stoica, O. Echavarren, A. M. Rh-Catalyzed Ortho C–H Alkynylation of Aromatic Aldehydes. *Org. Lett*. **23**, 1263–1268 (2021).

16. Liu, T.; Qiao, J. X.; Poss, M. A.; Yu, J.-Q. Palladium(II)-Catalyzed Site-Selective C(sp3)–H Alkynylation of Oligopeptides: A Linchpin Approach for Oligopeptide–Drug Conjugation. *Angew. Chem. Int. Ed*. **56**, 10924–10927 (2017).

17. (a) Xie, J., Shi, S., Zhang, T., Mehrkens, N., Rudolph, M., Hashmi, A. S. K. A Highly Efficient Gold-Catalyzed Photoredox a-C(sp^3)-H Alkynylation of Tertiary Aliphatic Amines with Sunlight. *Angew. Chem. Int. Ed*. **54**, 6046–6050 (2015). (b) Xu, H., Chen, R., Ruan, H., Ye, R., Meng, L. G. Visible-Light-Promoted Formation of C-C and C-P Bonds Derived from Evolution of Bromoalkynes under Additive-FreeConditions: Synthesis of 1,1-Dibromo-1-en-3-ynesandAlkynylphosphine Oxides. *Chin. J. Chem.* **39**, 873-878 (2021). (a) Xie, X., Liu, J., Wang, L., Wang, M. Visible-Light-Induced Alkynylation of α-C–H Bonds of Ethers with Alkynyl Bromides without External Photocatalyst. *Eur. J. Org. Chem.* 1534–1538 (2020).

Methods Summary

Photo-induced rhodium catalyzed *ortho*-alkynylation of arenes.

In an oven-dried screw capped reaction tube was charged with magnetic stir-bar, 8-aryl quinoline (0.1 mmol), $[Rh(COD)Cl]_2$ (5 mol%), KH_2PO_4 (0.2 mmol, 2.0 equiv). The vial was capped and wrapped with a Teflon seal. After that (bromoethynyl)triisopropylsilane (0.3 mmol, 3.0 equiv) was added with a microlitre pipette and 1 mL acetic acid was added with a disposable laboratory syringe under nitrogen condition. The reaction tube was placed 3 cm away from 34 W Kessil lamp with stirring (1000 rpm) for 24 h. The temperature was maintained at approximately (30-35 ^oC) through cooling with a fan. Upon completion the mixture was diluted with ethyl acetate and filtered through a celite pad. The filtrate was evaporated under reduced pressure and the crude mixture was purified by column chromatography using silica (100-200 mesh size) and petroleum ether / ethyl acetate as the eluent.

Data availability

Experimental data as well as characterization data for all the compounds prepared in the course of these studies are provided in the Supplementary Information of this manuscript. The X-ray crystallographic coordinates compounds 1 and 14 have been deposited at the Cambridge Crystallographic Data Center (CCDC) with accession codes 2103199 and 2168677 respectively. These data can be obtained free of charge from the Cambridge Crystallographic Data Center via www.ccdc.cam.ac.uk/structures/.

Declarations

Acknowledgements

Financial support received from SERB TETRA is gratefully acknowledged (TTR/2021/000108). Financial support re-ceived from CSIR-India (fellowship to A.S., A.G.), and IIT Bombay (S.G., D.K.M., SP., A.M.) is gratefully acknowledged.

Author contributions

A.S., A.G., S.G., D.M. conceived the concept. A.S., A.G., D.K.M., A.M. performed the reactions and analyzed the products. A.S., A.G., S.G., D.M. designed the control experiments and mechanistic pathway. S.P. carried out the computational studies. The manuscript was written through contributions of all authors. All authors have given approval to the final version of the manuscript.

Competing interests: The authors declare no competing interest(s).

Additional information

Supplementary Information is linked to the online version of the paper at www.nature.com/nature

Reprints and permissions information is available at www.nature.com/reprints. Readers are welcome to comment on the online version of this article at www.nature.com/nature.

Correspondence and requests for materials should be addressed to D.M. (dmaiti@iitb.ac.in).

Figures

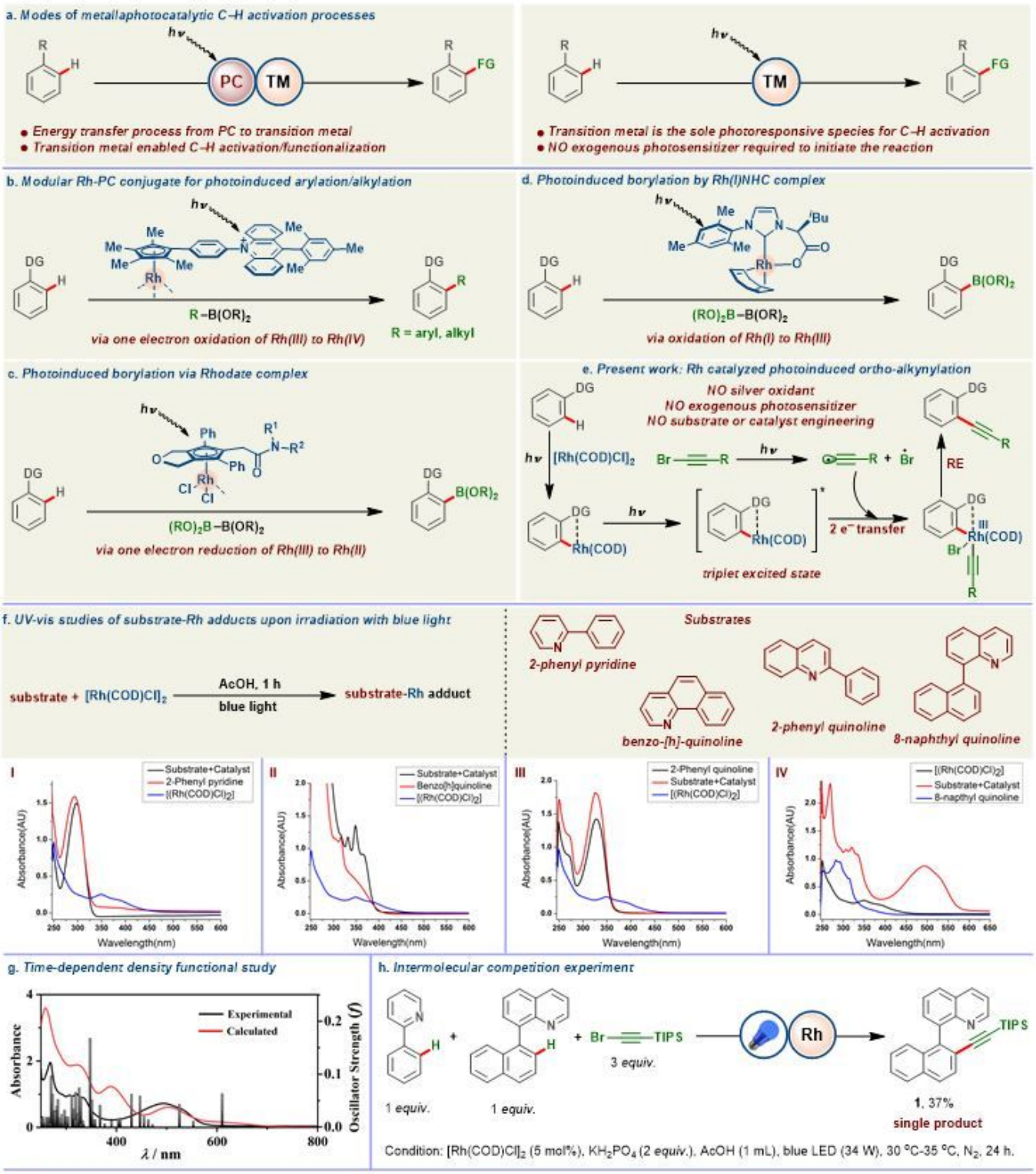

Figure 1

The realm of metallaphotocatalytic C-H activation strategies. **a**, Different modes of metallaphotocatalytic C-H activation. **b**,. Rh-PC modular conjugate for photo-induced *ortho*-C-H arylation and alkylation. **c**,. Photo-induced *ortho*-C-H borylation by *in situ* generated Rh(II) complex. **d**, Rh-NHC complex promoted *ortho*-C-H borylation. **e**, Rh-substrate cooperativity in promoting *ortho*-C-H alkynylation. **f**, UV-vis study for the Rh-substrate adduct. **g**, Experimental and TD-DFT calculated (at M06-L/TZVP/SDD(SMD/CH_3COOH))

electronic spectra of representative $[Rh(COD)Cl]_2$ + substrate]. Oscillator strengths are shown by the black vertical lines; the spectra (red) are convoluted with a Gaussian function having full width at half-maximum of 3000 cm^{-1}. **h**, Intermolecular competition experiment for five- vs six-membered metallacycle.

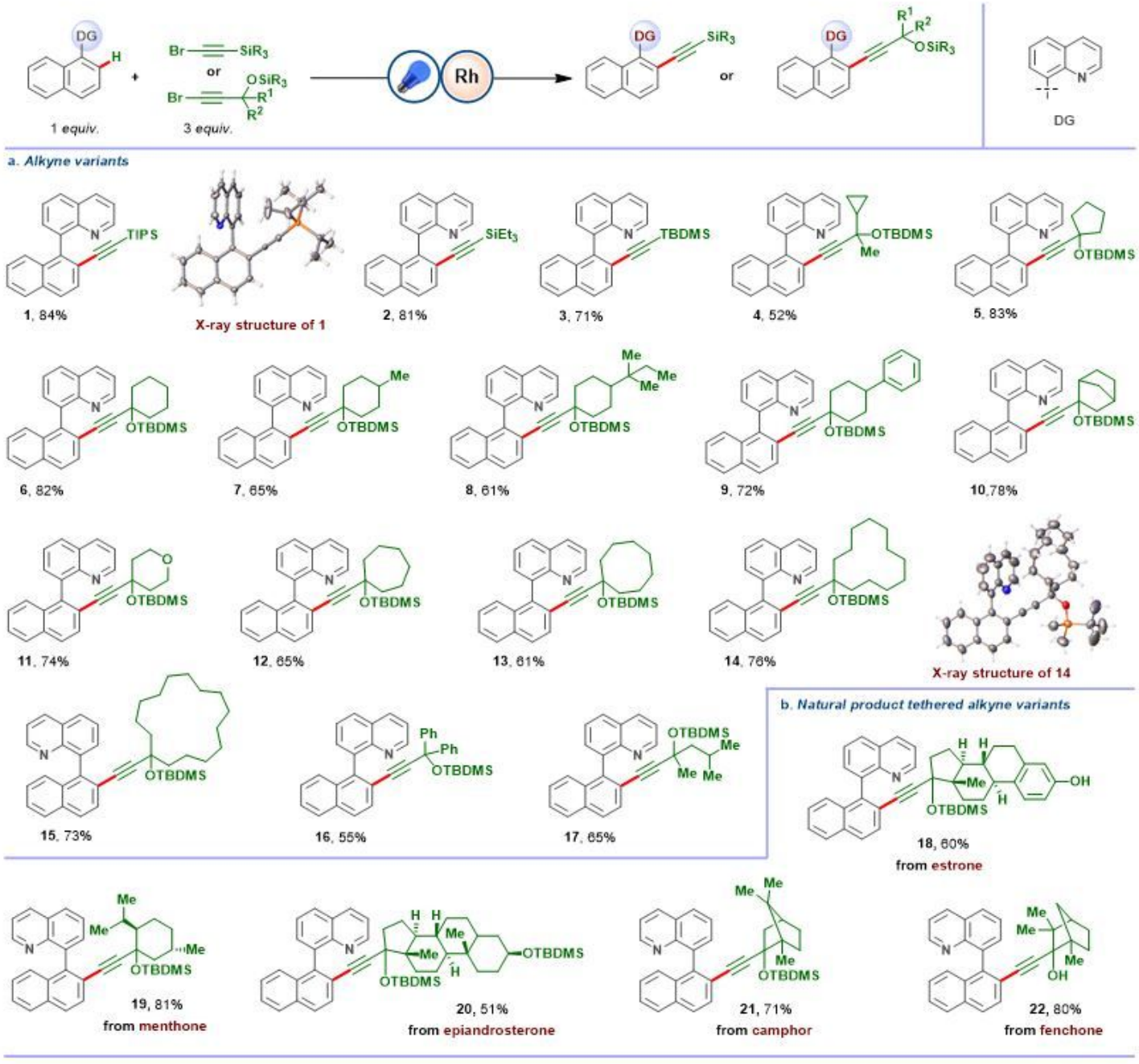

Figure 2

Photoinduced alkynylation of 8-naphthylquinoline with different alkyne variants. **1**-**22**: Reaction conditions: $[Rh(COD)Cl]_2$ (5 mol%), KH_2PO_4 (2 equiv.), AcOH (1 mL), blue LED (34 W), 30 ^oC-35 ^oC, N_2, 24 h. Isolated yields are reported.

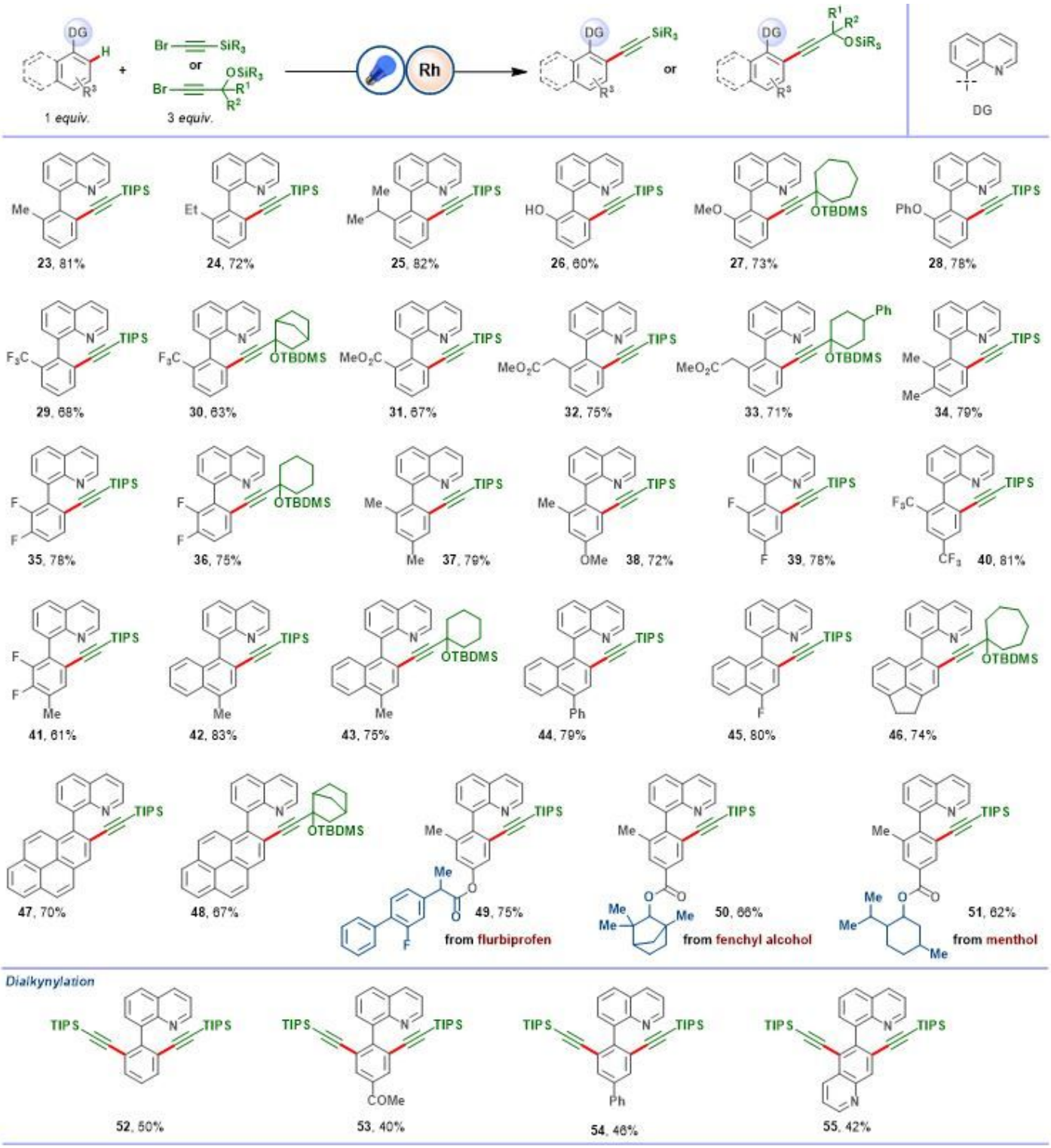

Figure 3

Photoinduced *ortho*-alkynylation of diverse arenes. **23-55**: Reaction conditions: $[Rh(COD)Cl]_2$ (5 mol%), KH_2PO_4 (2 equiv.), AcOH (1 mL), blue LED (34 W), 30 ^oC-35 ^oC, N_2, 24 h. 52-55: alkynyl bromide (6 equiv.). Isolated yields are reported.

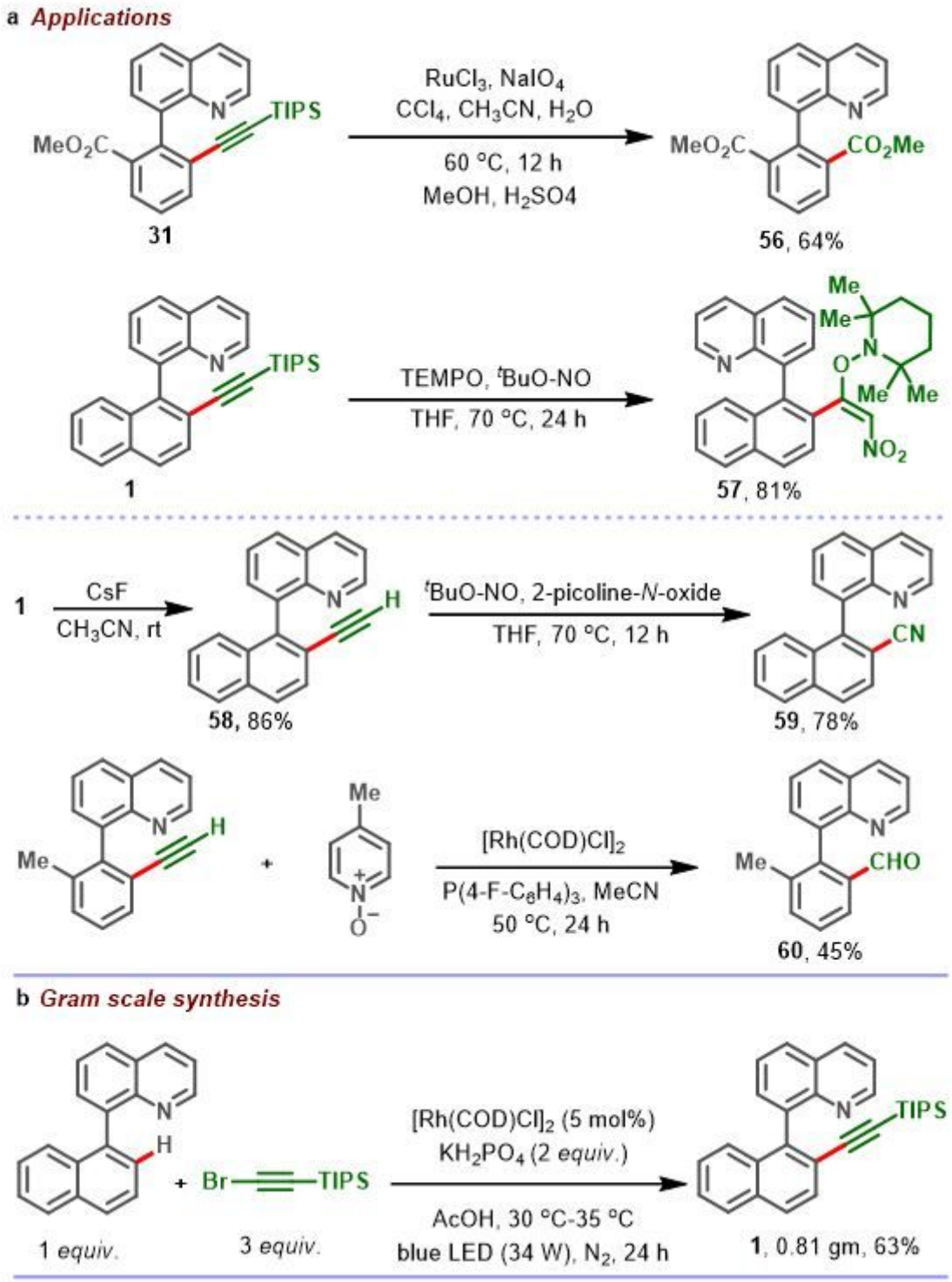

Figure 4

Applicative potential for photo-induced *ortho*-alkynylation of arenes.

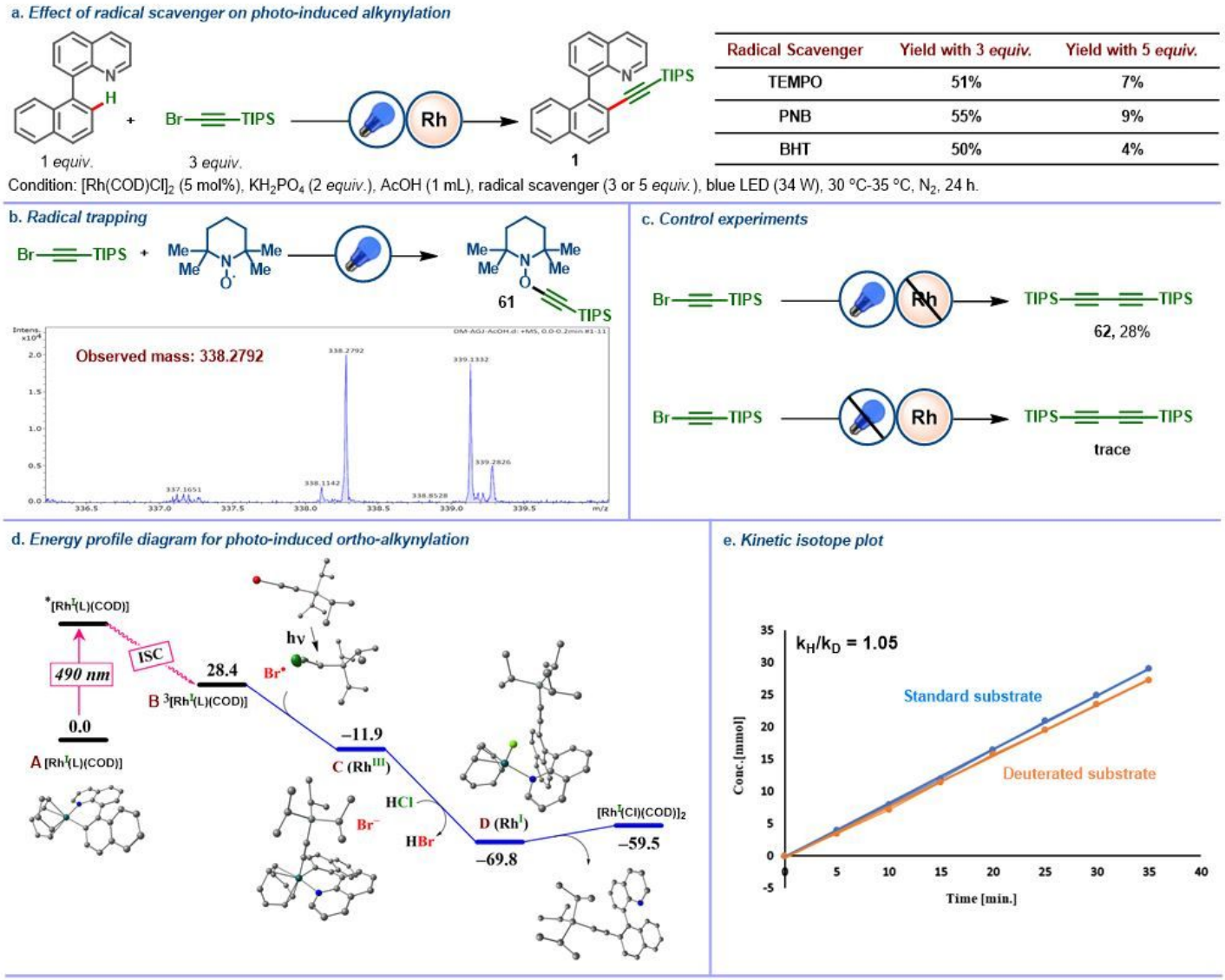

Figure 5

Mechanistic aspects of photoinduced *ortho*-alkynylation of arenes. a, Effect of radical scavenger on photo-induced *ortho*-C-H alkynylation. **b,** Radical trapping experiment of alkynyl radical. **c,**. Control experiments to depict the role of light in homolysis of alkynyl bromide **d,** Computed Gibbs free energies profile (in kcal/mol) for the photo-induced alkynylation of 8-(naphthalen-1-yl)quinoline (L) at the M06L(SMD)/TZVP/SDD//B3LYP/6-31G**/LANL2DZ level. Population of spin on the alkynyl radical is shown as green isosurface. **e,** Kinetic isotope plot

Supplementary Files

This is a list of supplementary files associated with this preprint. Click to download.

- SupplementaryInformation.pdf
- checkcifDMAGS187B.pdf

- checkcifDMAJASOrgMo.pdf
- DMAJASOrgMo.cif
- DMAGS187B.cif